CHEMISTRY

A general strategy to synthesize chemically and topologically anisotropic Janus particles

Jun-Bing Fan,[1] Yongyang Song,[1,2] Hong Liu,[3] Zhongyuan Lu,[3] Feilong Zhang,[2,4] Hongliang Liu,[1] Jingxin Meng,[1] Lin Gu,[5] Shutao Wang,[1,2]* Lei Jiang[1,2]

Emulsion polymerization is the most widely used synthetic technique for fabricating polymeric particles. The interfacial tension generated with this technique limits the ability to tune the topology and chemistry of the resultant particles. We demonstrate a general emulsion interfacial polymerization approach that involves introduction of additional anchoring molecules surrounding the microdroplets to synthesize a large variety of Janus particles with controllable topological and chemical anisotropy. This strategy is based on interfacial polymerization mediated by an anchoring effect at the interface of microdroplets. Along the interface of the microdroplets, the diverse topology and surface chemistry features of the Janus particles can be precisely tuned by regulating the monomer type and concentration as well as polymerization time. This method is applicable to a wide variety of monomers, including positively charged, neutrally charged, and negatively charged monomers, thereby enriching the community of Janus particles.

INTRODUCTION

In nature, biological particles with highly anisotropic chemistries and topologies, such as neurons (*1*), bacteriophages (*2*), and hemoglobin (*3*, *4*), play important roles in the activities of life (*5*). Learning from nature, scientists have aimed to synthesize particles that mimic these natural particles because of their great potential for fundamental research and practical applications in cancer diagnostics (*6*), self-assembled biomaterials (*7*–*9*), smart micromachines (*10*, *11*), and energy transporters (*12*). Emulsion polymerization, as a traditionally leading synthesis technique, has been widely used for the synthesis of polymeric particles (*13*–*15*). However, spherical particles are often formed because of interfacial tension (*16*, *17*), which limits flexibility in tuning the topology and chemistry of the particles (*18*–*22*). Achieving large-scale synthesis of uniform Janus particles with tunable topology and surface chemistry by emulsion polymerization remains a great challenge. Here, we demonstrate a general emulsion interfacial polymerization approach, which can be scaled up to synthesize a large variety of Janus particles with uniform topology, narrow size distribution, and variability in topology and chemistry.

RESULTS

Rational interfacial design for the large-scale synthesis of Janus particles with tunable topology and surface chemistry

In designing our method, we hypothesized that a dynamic interfacial reaction could be harnessed to break the spherical limitation, such as by making the interfacial reaction start from a specific point rather than from the entire spherical interface of the microdroplets. Here, we attempted to synthesize anisotropic particles by introducing additional anchoring molecules into the interface of the microdroplets. As a proof of concept, we chose to use a typical oil-in-water emulsion system, styrene (St) and divinylbenzene (DVB) in water emulsion, into which, as an example, hydrophilic acrylic acid (AA) was introduced as anchoring molecules. Briefly, when 7 mmol AA anchoring molecules are introduced outside St/DVB-based (13 mmol St, 7 mmol DVB) droplets, they can polymerize to form Janus poly(styrene-*co*-divinylbenzene) ⊃ poly(acrylic acid) (PSDVB ⊃ PAA) particles with a crescent moon topology and amphiphilicity (the symbol "⊃" represents the orientation of the hydrophobic concave surface and hydrophilic convex surface of the Janus particles). These particles have average diameters of 2.31 ± 0.16 μm and "opening degree" of 104.1 ± 14.5° (the opening degree can be defined as a central angle of sector that corresponds to the concave region of the Janus particle). In contrast, in the absence of AA, the polymerization produced only the spherical particles typical of traditional methods of emulsion polymerization (fig. S1). Energy-dispersive x-ray (EDX) spectroscopy analysis revealed distinct O distribution on the convex/concave surfaces of the particles. For the PSDVB ⊃ PAA particles, the O element only existed in the PAA, implying that the convex surface of the particle was hydrophilic PAA, whereas the concave surface was hydrophobic PSDVB (Fig. 1A). Aberration-corrected scanning transmission electron microscopy (STEM) images of the embedded particles, after microtome sectioning and staining with phosphotungstic acid, revealed two layers. The thickness of the PAA layer in the Janus particles was 53 ± 20 nm (Fig. 1B). When polymerization was scaled up to three times the aforementioned monomer feed, this approach produced uniform Janus particles of approximately 5 g in one batch, providing an effective way to synthesize Janus particles on a large scale. These results demonstrate that the introduction of anchoring molecules can successfully produce Janus particles with hydrophilic convex surfaces and hydrophobic concave surfaces.

We next investigated the influence of concentration of the anchoring molecules and hydrophobic monomers on the topology of the Janus particles. At low AA concentrations of 0.06 M, bread-shaped Janus particles were easily formed. As the concentration of AA increased, the anisotropic topology of the Janus particles gradually changed from bread-shaped to hemispherical-, crescent moon–, and even pistachio-shaped particles at a high AA concentration of 0.3 M (Fig. 1C). When the concentration of AA was further increased, a composite film could be

[1]CAS Key Laboratory of Bio-inspired Materials and Interfacial Science, CAS Center for Excellence in Nanoscience, Technical Institute of Physics and Chemistry, Chinese Academy of Sciences, Beijing 100190, P. R. China. [2]University of Chinese Academy of Sciences, Beijing 100049, P. R. China. [3]State Key Laboratory of Supramolecular Structure and Materials, Institute of Theoretical Chemistry, Jilin University, Changchun 130023, P. R. China. [4]Beijing National Laboratory for Molecular Sciences, Institute of Chemistry, Chinese Academy of Sciences, Beijing 100190, P. R. China. [5]Beijing National Laboratory for Condensed Matter Physics, Institute of Physics, Chinese Academy of Sciences, Beijing 100190, P. R. China.
*Corresponding author. Email: stwang@mail.ipc.ac.cn

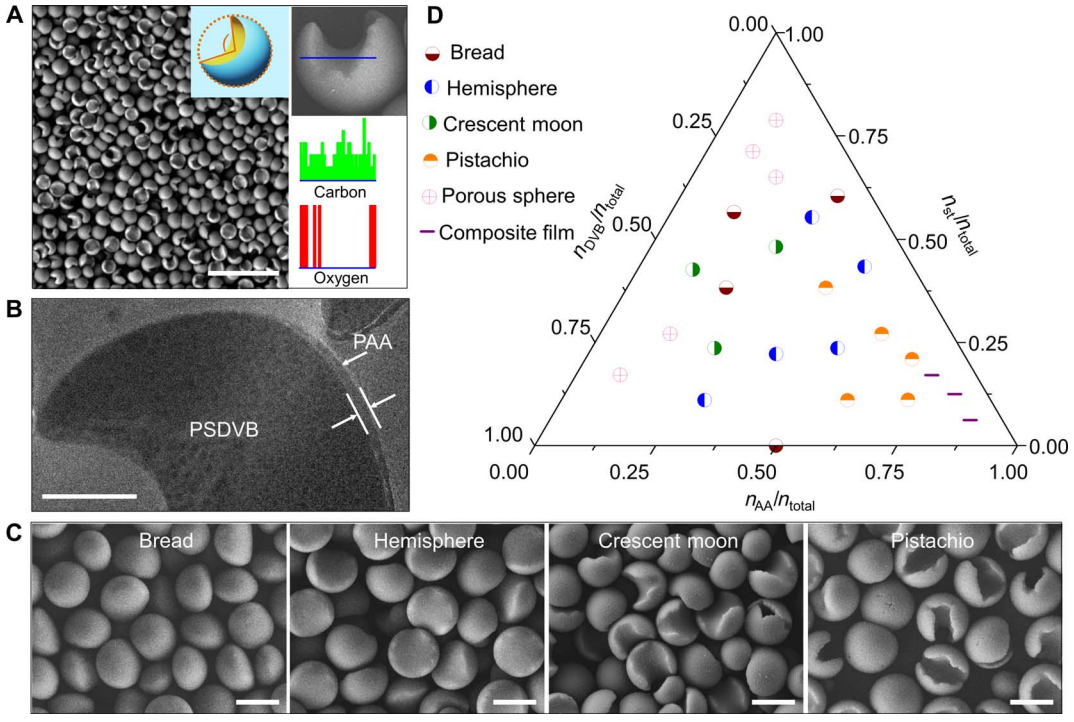

Fig. 1. Synthesis and characterization of the Janus particles. (**A**) High-yield synthesis of typical crescent moon–shaped PSDVB ⊃ PAA Janus particles. The resulting crescent moon–shaped Janus particles exhibited a uniform size. Inset: The opening degree describes the topology features of the Janus particle. The opening degree can be defined as a central angle of sector that corresponds to the concave region of the Janus particle. Scale bar, 10 μm. The EDX spectroscopy analysis indicated different O element distributions on the convex and concave surfaces of the Janus particle. The O element was only observed in PAA, indicating that the convex surface of the particle was hydrophilic PAA, whereas the concave surface was hydrophobic PSDVB. (**B**) STEM image of embedded Janus particles after microtome cutting and staining with phosphotungstic acid. Scale bar, 500 nm. (**C**) Scanning electron microscopy (SEM) images of topologically anisotropic Janus particles. The topological geometries of the Janus particles could be well tuned to sequentially achieve bread, hemisphere, crescent moon, and pistachio topologies by regulating the concentrations of the anchoring monomer. Scale bar, 2 μm. (**D**) Ternary phase–like diagram of AA, St, and DVB for the production of the topologically anisotropic Janus particles. Janus particles were obtained using molar ratios of $n_{St}/n_{total} < 0.625$, $n_{DVB}/n_{total} < 0.625$, and $n_{AA}/n_{total} < 0.75$.

obtained, as shown in the ternary phase diagram of AA, St, and DVB (Fig. 1D). Regarding the hydrophobic monomers, when the amount of St or DVB increased, the topology of resultant particles changed from Janus particles (bread, hemisphere, and crescent moon) to porous particles. Bread- and hemispherical-shaped particles were easily produced at molar ratios of $n_{St}/n_{total} < 0.625$, $n_{DVB}/n_{total} < 0.625$, and $0.1 < n_{AA}/n_{total} \leq 0.5$. Crescent moon–shaped particles were formed at molar ratios of $0.25 < n_{St}/n_{total} < 0.5$, $0.25 < n_{DVB}/n_{total} < 0.5$, and $0.1 < n_{AA}/n_{total} \leq 0.25$. Pistachio-shaped particles were easily produced at molar ratios of $0.1 < n_{St}/n_{total} < 0.5$, $n_{DVB}/n_{total} < 0.25$, and $0.35 < n_{AA}/n_{total} < 0.75$ (Fig. 1D). Outside these ranges, spherical porous particles and composite films were produced (fig. S2). Notably, the chemical anisotropy with respect to the amphiphilicity and surface charge of the Janus particles also changed along with their topologies. Therefore, addition of anchoring molecules during emulsion interfacial polymerization can effectively control the topology and surface chemistry features of Janus particles.

The formation mechanism of the Janus particles by emulsion interfacial polymerization

To explore the formation mechanism of Janus particles, we carefully observed the growth process at different polymerization times using optical microscopy and fluorescence microscopy (Fig. 2 and fig. S3). After polymerization proceeded for 15 min, a particle that underwent Brownian motion was observed inside the droplet (Fig. 2, B and C, movie S1; 15 min). This is because the free radicals from water-insoluble 2,2′-azobisisobutyronitrile (AIBN) were initially generated inside the droplet and subsequently initiated the polymerization of the hydrophobic St and DVB (Fig. 2A). The particle occasionally collided toward the interface of the droplet, although the precise mechanism is currently unclear. After the particle arrived at the interface of the droplet, the hydrophilic anchoring monomers could interact with the particle and then be initiated to polymerize, rendering the particle anchored at the interface of the droplet and triggering interfacial anchoring polymerization (Fig. 2, B and C; 30 min). Finally, the particle was trapped at the interface of the droplet because of the anchoring effect. Therefore, the subsequent polymerization occurred primarily along the interface of the droplets, resulting in the interfacial preferential growth of the particles (Fig. 2, B and C; 45 and 65 min). The preferential growth of the particle at the interface is based on the equal chemical potential between hydrophobic phases and hydrophilic phases at equilibrium. For the system comprising two immiscible monomer phases at equilibrium, the chemical potential of the hydrophobic phase was equal to that of the chemical potential of hydrophilic phase (*23*–*26*). The particle grew at the interface as a result of the increased chemical potential. Until the next new equilibrium appeared, the difference in the chemical potential between hydrophobic phase and hydrophilic phase was again equal to zero. Therefore, to maintain the chemical potential being equal to each other, the polymerization of the monomers at the interface of the droplets was inevitably favored over polymerization at other regions. In this case, the most stable state for the preferential growth of the particles at

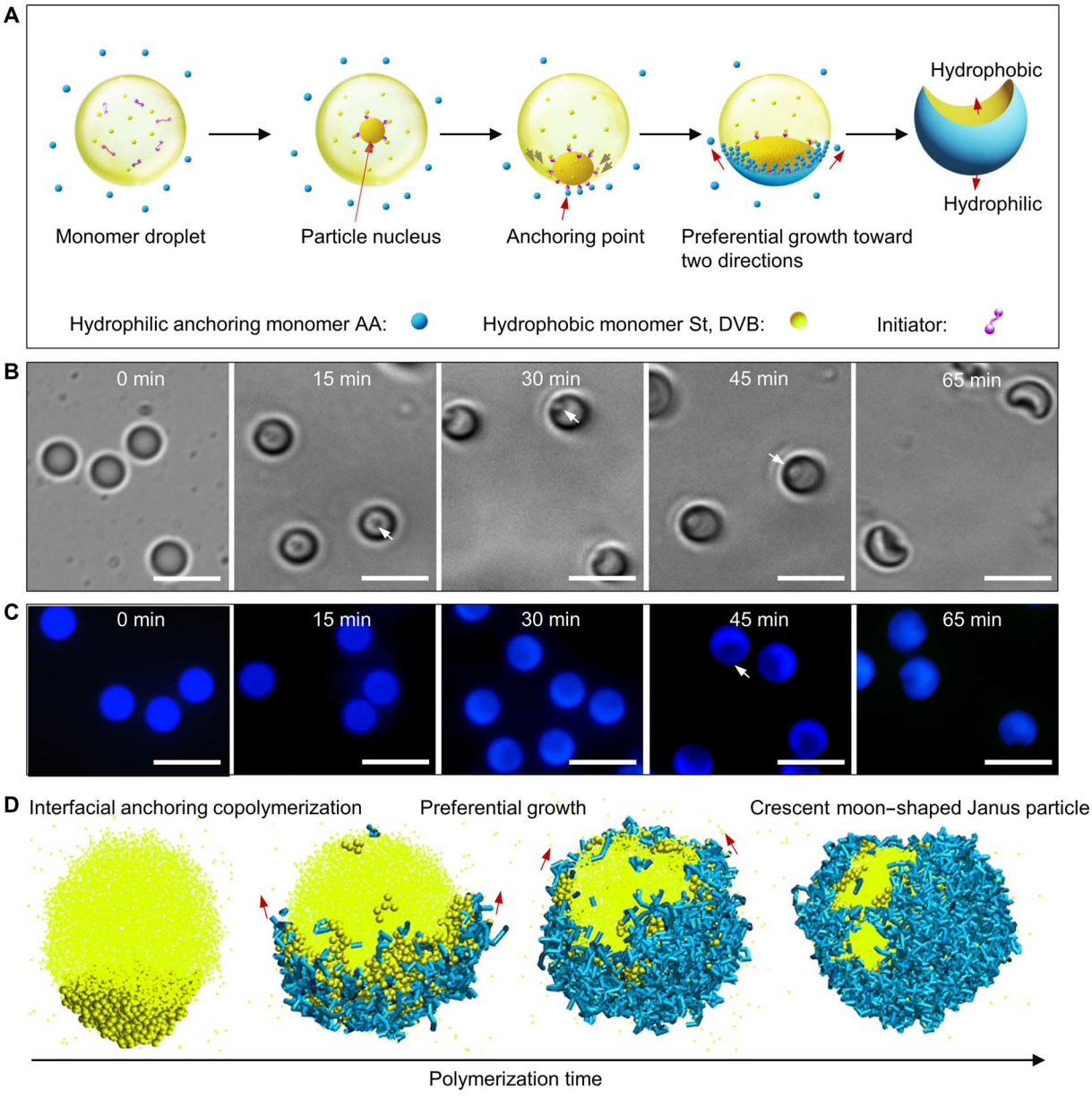

Fig. 2. Emulsion interfacial polymerization mechanism for producing Janus particles. (**A**) Schematic of the fabrication of Janus particles. The initial polymerization of hydrophobic monomers inside the droplet could produce a particle nucleus that moved toward the oil/water interface. In this case, the hydrophilic anchoring monomers in the external water phase could contact the particle nucleus and be initiated to polymerize, thereby anchoring the particle at the interface of the droplet, triggering interfacial anchoring polymerization. Subsequently, based on the equal chemical potential principle at equilibrium, preferential copolymerization of AA, St, and DVB occurred along the interface in two directions, resulting in the formation of crescent moon–shaped Janus particles. (**B**) Bright-field microscope images of the time-dependent growth process of Janus particles. Scale bar, 5 μm. (**C**) Fluorescence microscope images of the time-dependent growth process of Janus particles. Scale bar, 5 μm. (**D**) Computer simulation results. A dissipative dynamic simulation model combined with a stochastic reaction model was constructed to investigate the dynamic behavior during the interfacial polymerization. The yellow bead represents the St and DVB, whereas the blue sticks represent the polymerized AA monomers. Here, the AA anchoring monomers in the aqueous phase are not shown for clarity. The simulation consistently suggested preferential growth along two directions at the interface, which led to the formation of Janus particles similar to those obtained in the experiment.

the interface may be growth in two directions rather than uniform growth around the interface. Therefore, further preferential growth along the two directions of the interface led to the formation of Janus particles instead of spherical particles.

To better understand this dynamic emulsion interfacial polymerization, we constructed a dissipative dynamics simulation model combined with a stochastic reaction model (see the Supplementary Materials for more details) (*27*–*35*). As shown in Fig. 2D, starting from the particle (colored deep yellow), the interfacial anchoring polymerization occurred between the hydrophobic monomers inside microdroplets and external hydrophilic anchoring monomers (figs. S4 and S5). The simulation consistently indicated the preferential growth of the particle along the two directions of the interface (Fig. 2D), in agreement with the experiments. Our simulation also demonstrated that the

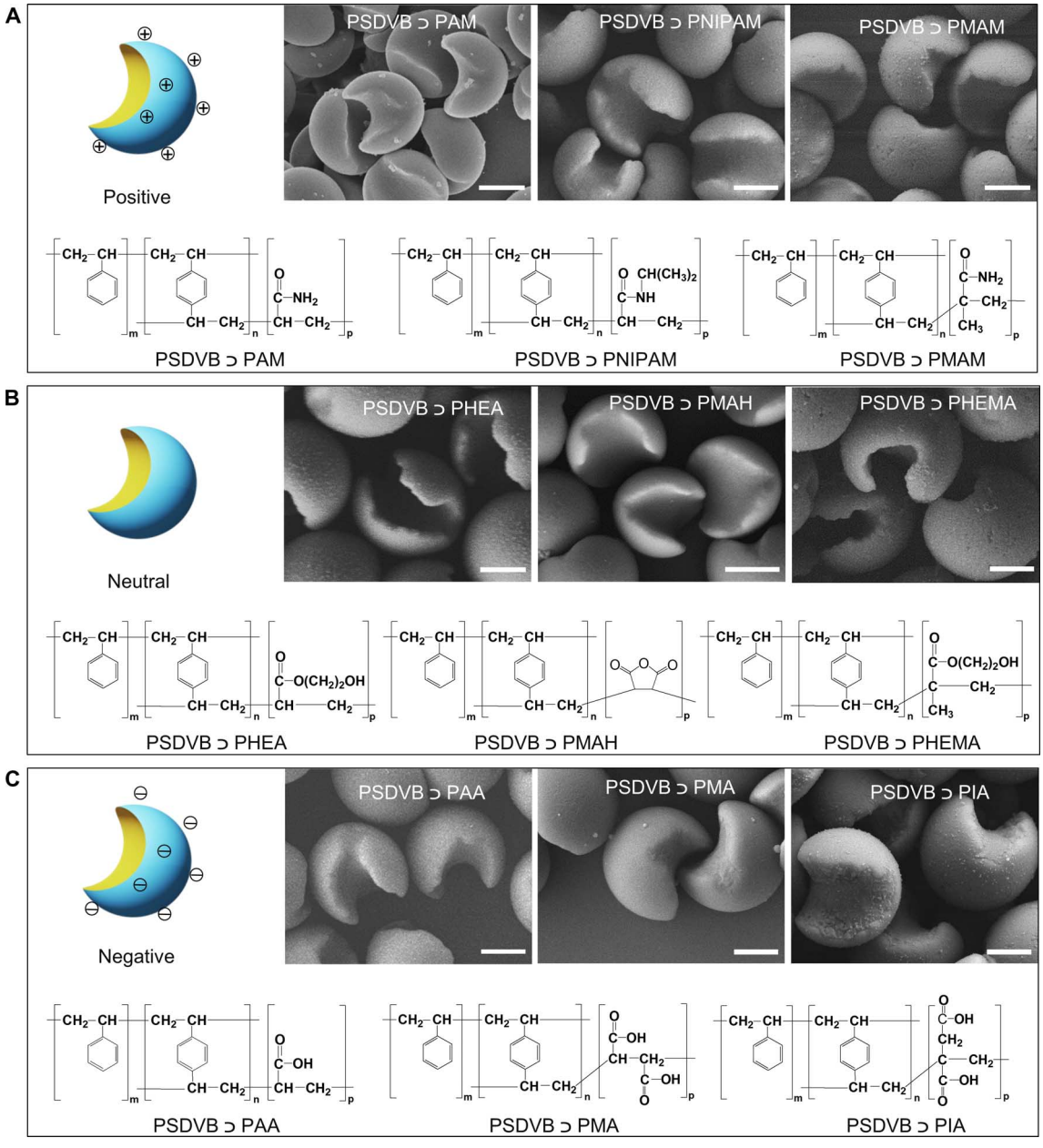

Fig. 3. Community of Janus particles. (**A**) Positively charged Janus particles. (**B**) Neutrally charged Janus particles. (**C**) Negatively charged Janus particles. The emulsion interfacial polymerization is applicable to a wide variety of monomers, greatly enriching the community of Janus particles. Scale bar, 1 μm.

topology of the Janus particle was strongly dependent on the concentration of the hydrophilic anchoring monomers and hydrophobic monomers. As expected, with an increasing concentration of hydrophilic anchoring monomers, hemispherical-, crescent moon–, and pistachio-shaped Janus particles were observed in sequential order (fig. S6), similar to the experimental results. At low concentrations, a small amount of hydrophilic anchoring monomers could not continuously afford polymerization along the interface; thus, bread- or hemispherical-shaped Janus particles were obtained. At high concentrations, sufficient anchoring monomers were continually supplied to polymerize along the interface, enabling the formation of crescent moon–shaped, even pistachio-shaped, Janus particles. Furthermore, the topologies of the particles changed from hemispherical-shaped to crescent moon–shaped and finally to spherical particles with increasing the number of hydrophobic monomers. The polymerization of hydrophobic monomers forms the inner layer of the particle. When the number of hydrophobic monomers is low, the formation of the inner layer along the interface is difficult, thus facilitating the formation of Janus particles. By contrast, when the number of hydrophobic monomers is sufficient, the inner layer can grow synchronously with the interfacial layer, finally forming spherical particles (fig. S7).

The generality of emulsion interfacial polymerization for the synthesis of Janus particles

The emulsion interfacial polymerization strategy was further expanded to the polymerization of other vinyl monomers. We used different

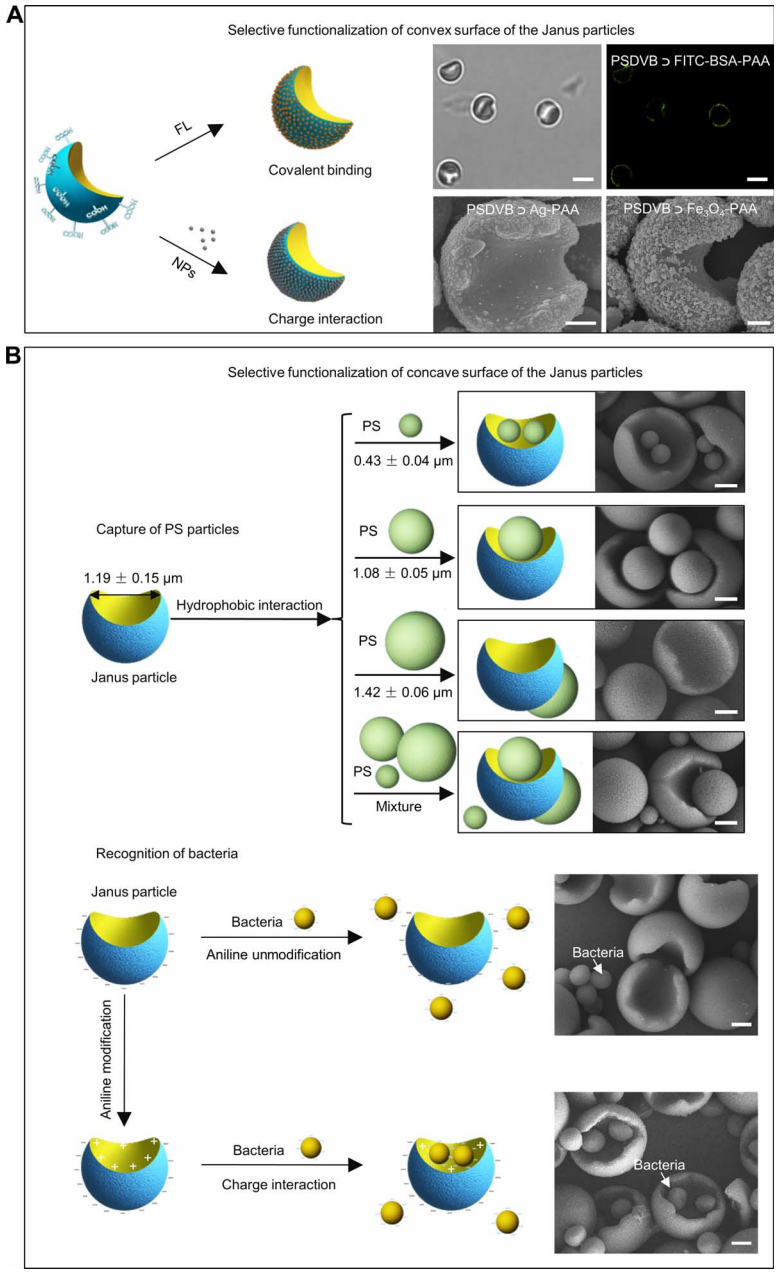

Fig. 4. Selective surface functionalization of the Janus particles. (**A**) Selective functionalization of the convex surface of the Janus particles. The fluorescent FITC-BSA molecules were selectively modified onto the convex surface of the PSDVB ⊃ PAA Janus particles. Scale bar, 2 μm. Meanwhile, inorganic nanoparticles, such as Ag and Fe_3O_4 nanoparticles, were also locked onto the convex surface of the Janus particles via one-step electrostatic attraction. Scale bar, 500 nm. (**B**) Selective functionalization of the concave surface of the Janus particles. Janus particles were used to capture and recognize spherical PS particles and live bacteria (*S. aureus*). When the PSDVB ⊃ PAA Janus particles were mixed with spherical PS particles with diameters of 0.43 ± 0.04 μm, 1.08 ± 0.05 μm, and 1.42 ± 0.06 μm, respectively, those with diameters of 0.43 ± 0.04 μm and 1.08 ± 0.05 μm were captured on the concave surfaces, whereas those with diameters of 1.42 ± 0.06 μm were difficult to capture. When the PSDVB ⊃ PAA Janus particles were simultaneously mixed with PS particles with three different particle sizes, the PS spheres with average diameters of 1.08 ± 0.05 μm were the more easily captured particles. Meanwhile, the concave surfaces of the Janus particles functionalized by aniline were used to selectively recognize live bacteria through electrostatic interactions. Scale bar, 500 nm.

anchoring monomers, including positively charged, neutrally charged, and negatively charged monomers, to surround the St/DVB-based droplets. A large variety of Janus particles with crescent moon structures were produced, indicating the generality of this strategy (Fig. 3 and figs. S8 to S15). This approach yielded well-defined Janus particles of poly(styrene-*co*-divinylbenzene) ⊃ poly(acrylamide) (PSDVB ⊃ PAM), poly(styrene-*co*-divinylbenzene) ⊃ poly(*N*-isopropylacrylamide) (PSDVB ⊃ PNIPAM), poly(styrene-*co*-divinylbenzene) ⊃ poly(methacrylamide) (PSDVB ⊃ PMAM) (Fig. 3A), poly(styrene-*co*-divinylbenzene) ⊃ poly(hydroxyethyl acrylate) (PSDVB ⊃ PHEA), poly(styrene-*co*-divinylbenzene) ⊃ poly(maleic anhydride) (PSDVB ⊃ PMAH), poly(styrene-*co*-divinylbenzene) ⊃ poly(hydroxyethyl methacrylate) (PSDVB ⊃ PHEMA)

(Fig. 3B), PSDVB ⊃ PAA, poly(styrene-*co*-divinylbenzene) ⊃ poly(maleic acid) (PSDVB ⊃ PMA), and poly(styrene-*co*-divinylbenzene) ⊃ poly(itaconic acid) (PSDVB ⊃ PIA) (Fig. 3C). On the basis of these oil-in-water emulsion systems, a possible principle for this emulsion interfacial polymerization method should briefly meet three criteria: (i) The system could form a stable oil-in-water emulsion interface, (ii) the monomer pairs in the hydrophilic and hydrophobic phases should follow the same polymerization mechanism, and (iii) the initial polymerization should start in the oil phase.

Anisotropic functionalization of Janus particles and their applications

Beyond the inherent amphiphilicity of the Janus particles, these well-defined Janus particles could be rationally designed to realize selective surface functionalization. On the one hand, the convex surface of the Janus particles could be modified with "patch" molecules or nanoparticles by covalent or noncovalent bonding (Fig. 4A). For example, fluorescent fluorescein isothiocyanate (FITC)–bovine serum albumin (BSA) was selectively grafted onto the convex surface of the Janus PSDVB ⊃ PAA particles through a condensation reaction between the carboxyl groups and amino groups. Moreover, by exploiting the electronegative properties of PAA at the convex surface of the PSDVB ⊃ PAA Janus particles, we decorated positively charged inorganic nanoparticles, such as Ag (fig. S16) and Fe_3O_4 nanoparticles (fig. S17), onto the convex surface via charge interactions, resulting in multifunctional Janus particles. On the other hand, the concave surface of the Janus particles could also be effectively used. For example, Janus particles were used to capture spherical polystyrene (PS) particles to realize shape complementarity. When the Janus particles with concave diameters of 1.19 ± 0.15 μm were respectively mixed with spherical PS particles with diameters of 0.43 ± 0.04 μm, 1.08 ± 0.05 μm, and 1.42 ± 0.06 μm, many PS particles with diameters less than the concave diameters of Janus particles were trapped in their concaves because of hydrophobic interactions, except for the 1.42-μm-diameter particles. However, when the Janus particles were simultaneously mixed with all three PS particles, the PS particles with diameters of 1.08 ± 0.05 μm were more favorable for capture under current conditions (Fig. 4B and fig. S18, A to D). In addition, concave surfaces of Janus particles functionalized with aniline were used to selectively recognize live bacteria (*Staphylococcus aureus*; size, approximately 600 nm), whereas unmodified particles were difficult for this recognition (Fig. 4B and fig. S18, E and F). Functionalizing the concave surfaces of the Janus particles made the concave surfaces positively charged; consequently, they could attract bacteria with negative charges. Moreover, the negatively charged convex surfaces of the Janus particles could repel bacteria. The unique surface charge properties of the Janus particles and their concave sizes enabled them to effectively recognize live bacteria. Therefore, selectively modifying the convex/concave surfaces of Janus particles may endow Janus particles with more functionality (*36*, *37*).

DISCUSSION

Janus particles with two distinct physical or chemical properties in their surfaces, like the two-faced Roman god Janus, are of importance in fundamental research and practical applications, such as self-assembly superstructures (*38*, *39*), bioimaging and therapeutics (*40*), solid surfactants (*41*), panel displays (*42*), micromotors (*43*, *44*), and optical probes (*45*). Achieving these applications is largely due to the anisotropic topology and surface chemistry of Janus particles. However, existing strategies, such as the particle self-assembly technique combined with shading modification (*46*), microfluidics (*41*), electrodynamic co-jetting (*47*), block copolymer self-assembly (*48*), and swelling emulsion polymerization (*23*), are still difficult for large-scale synthesis of uniform Janus particles with tunable topology and surface chemistry (*49*).

Our general emulsion interfacial polymerization method can effectively synthesize chemically and topologically anisotropic Janus particles in large scale. This method is in stark contrast to traditional emulsion polymerization methods that produce spherical particles or "snowman-shaped" or "dumbbell-shaped" particles. The emulsion interfacial polymerization system has several distinct advantages over traditional emulsion polymerization. (i) Emulsion interfacial polymerization overcomes the limitations of traditional emulsion polymerization. When additional anchoring molecules are introduced outside the microdroplets, polymerization starting from one specific point of the interface can break the uniform growth of particles at the entire interface of the droplets, resulting in the formation of chemically and topologically anisotropic Janus particles. (ii) Emulsion interfacial polymerization successfully overcomes the current challenges of achieving tunability of the chemical and topological anisotropy of synthetic particles. A wide range of Janus particles (bread, hemisphere, crescent moon, and pistachio) with chemical and topological anisotropy can be readily designed and realized through control of monomer type and concentration as well as polymerization time. (iii) Emulsion interfacial polymerization is general. The emulsion interfacial polymerization strategy can be used for polymerizing various vinyl monomers, including positively charged, neutrally charged, and negatively charged ones, greatly enriching the community of Janus particles. With respect to potential applications, we have demonstrated that these Janus particles exhibited remarkable abilities to separate bacteria by using their topological structures and surface chemistry. We strongly believe that our novel method will significantly expand the utility of Janus particles, creating new opportunities in a wide variety of applications, ranging from environment to health, especially in oil-water separation and biological detection.

MATERIALS AND METHODS

Synthesis and characterization of Janus particles

In a typical synthesis, 10 ml of a 1% (v/v) 1-chlorodecane (CD) oil-in-water emulsion containing 0.25% (w/v) SDS was mixed with 20 ml of an aqueous solution [containing 0.25% (w/v) SDS] of 1% (w/v) non–cross-linked PS particles at 40°C. The diameter of the PS particles used during polymerization was 1.08 ± 0.05 μm. After 16 hours of magnetic stirring, a 10-ml oil-in-water emulsion [containing 0.25% (w/v) SDS], composed of 13 mmol St, 7 mmol DVB, 0.24 mmol AIBN, and 7 mmol hydrophilic anchoring monomer AA, was prepared by ultrasonic emulsification, and it was subsequently added to the aforementioned solution at 40°C for 6 hours. After 5 ml of 1% (w/v) polyvinyl alcohol was added to the mixture followed by deoxygenation by bubbling with N_2 for 15 min at room temperature, the polymerization was performed at 70°C for 14 hours. All polymerizations were carried out in deionized water without using a co-solvent.

Characterization

Janus particles were prepared for SEM (7500, JEOL) by dropping 20 μl of particle aqueous solution onto a silicon wafer (1 cm × 1 cm) at room temperature. After water evaporation, the samples were coated with platinum using a vacuum evaporator for SEM images. The growth

process of the Janus particles was observed by using an optical microscope and fluorescence microscope with a 100× objective (Ti-E, Nikon). The slices of Janus particles sectioned by microtome were characterized using an aberration-corrected STEM (JEM-ARM200F).

Synthesis of charged inorganic nanocrystals

Synthesis of positively charged Ag nanoparticles

Nearly monodisperse Ag nanoparticles were synthesized in a one-step method (*50*). In a typical synthesis, 300 mg of $AgNO_3$ was added to a mixture of 20 ml of liquid paraffin and 5 ml of oleylamine. The mixture was deoxygenated by bubbling with N_2 for 20 min and then heated to 160°C for 10 hours. The color of the mixture solution changed from bright orange to brown to black with reaction time. The resulting nanoparticles were washed three times with ethanol. Finally, the resultant Ag nanoparticles were redispersed in ethanol to interact with the anisotropic particles.

Synthesis of positively charged Fe_3O_4 nanoparticles

Magnetic Fe_3O_4 nanoparticles were synthesized according to a previously described method (*51*). In a typical synthesis, 3 mmol $Fe(acac)_3$ was dissolved in 24 ml of benzyl ether and 6 ml of oleylamine. After deoxygenation by bubbling with N_2 for 20 min, the solution was heated for 1 hour at 110°C for dehydration and then heated to 250°C for 1 hour. After the reaction, the solution was cooled to room temperature. The resultant Fe_3O_4 nanoparticles were washed three times with ethanol. Finally, the resultant Fe_3O_4 nanoparticles were redispersed in ethanol to interact with the anisotropic particles. The inorganic nanoparticles were characterized by a TEM (JEM-2010).

Selective functionalization of Janus particles

FITC-BSA covalent-modified PSDVB ⊃ PAA particles

Four hundred milligrams of crescent moon–shaped PSDVB ⊃ PAA Janus particles were dispersed in 50 ml of deionized water. Next, 0.2 g of 1-ethyl-3-(3-dimethylaminopropyl)carbodiimide and 0.4 g of *N*-hydroxysuccinimide were added to the PSDVB ⊃ PAA Janus particle suspension at 35°C for 10 hours to activate the carboxyl groups of PAA. Finally, 10 mg of activated PSDVB ⊃ PAA particles was added to 10 ml of a 0.25% (w/v) FITC-BSA aqueous solution at 35°C for 10 hours under magnetic stirring. The resulting particles were centrifuged at 5000 rpm for 5 min and washed three times with deionized water.

Charge interaction between Ag nanoparticles and PSDVB ⊃ PAA Janus particles

A positively charged Ag nanoparticle suspension [0.5 ml of 0.5% (w/v)] was added to 0.5 ml of the 1% (w/v) PSDVB ⊃ PAA particle suspension under gentle stirring for 10 hours. The resultant hybrid particles were purified by using a centrifugation-dispersion process. Twenty microliters of ethanol was added to the aforementioned solution, and the resultant solution was centrifuged at 5000 rpm for 5 min. This process was repeated three times to completely remove the unlocked nanoparticles.

Charge interaction between Fe_3O_4 nanoparticles and PSDVB ⊃ PAA Janus particles

A positively charged Fe_3O_4 nanoparticle suspension [0.5 ml of 0.5% (w/v)] was added to 1 ml of the 1% (w/v) PSDVB ⊃ PAA particle suspension under gentle stirring for 10 hours. The resulting hybrid particles were purified by using a centrifugation-dispersion process. Twenty microliters of ethanol were added to the aforementioned particle solution, and the resultant solution was centrifuged at 5000 rpm for 5 min.

Janus particle capture of spherical PS particles

To capture spherical PS particles with diameters of 0.43 ± 0.04 μm, 10 μl of a PSDVB ⊃ PAA Janus particle suspension (1%, w/v) with 8 μl of a spherical PS particle suspension (0.023%, w/v) was dispersed in 20 μl of deionized water. The solution was then ultrasonicated for 5 min and subsequently used directly for SEM imaging.

To capture spherical PS particles with diameters of 1.08 ± 0.05 μm, 10 μl of a PSDVB ⊃ PAA Janus particle suspension (1%, w/v) with 8 μl of a spherical PS particle suspension (0.364%, w/v) was dispersed in 20 μl of deionized water. Then, the solution was ultrasonicated for 5 min and subsequently used directly for SEM imaging.

To capture spherical PS particles with diameters of 1.42 ± 0.06 μm, 10 μl of a PSDVB ⊃ PAA Janus particle suspension (1%, w/v) with 8 μl of a spherical PS particle suspension (1%, w/v) was dispersed in 20 μl of deionized water. Then, the solution was ultrasonicated for 5 min and subsequently used directly for SEM imaging.

To capture mixtures of spherical PS particles with different sizes, 7 μl of a PSDVB ⊃ PAA Janus particle suspension (1%, w/v) with 8 μl of 0.43 ± 0.04–μm PS particles (0.023%, w/v), 8 μl of 1.08 ± 0.05–μm PS particles (0.364%, w/v), and 8 μl of 1.42 ± 0.06–μm PS particles (1%, w/v) was dispersed in 20 μl of deionized water. The solution was then ultrasonicated for 5 min and subsequently used directly for SEM imaging.

Janus particle recognition of *S. aureus*

Bacterial strains and growth conditions

S. aureus were initially grown in sterile LB broth overnight, shaken at 150 rpm at 37°C, and harvested during logarithmic growth.

Aniline modification of Janus particles

Twenty milligrams of PSDVB ⊃ PAA particles was dispersed in 1 ml of aniline and shaken overnight at room temperature. The suspension was washed twice with deionized water and finally redispersed in 1 ml of water.

Recognition of S. aureus by aniline-modified Janus particles

Two milliliters of *S. aureus* in culture (ca. 1×10^{10} cells/ml) were mixed with 1 ml of aniline-modified PSDVB ⊃ PAA particles (20 mg/ml) under magnetic stirring for 24 hours at room temperature. In addition, the samples were rinsed with deionized water and filtered to remove salts and planktonic bacteria. The samples were then fixed in a 2.5% glutaraldehyde aqueous solution overnight at 4°C, after which they were rinsed with deionized water. Finally, the samples were dehydrated in a series of ethanol aqueous solutions (30, 50, 70, 85, and 95%), followed by two rinses in 100% ethanol. A control experiment with unmodified Janus particles was also carried out using the same procedures.

SUPPLEMENTARY MATERIALS

Supplementary material for this article is available at http://advances.sciencemag.org/cgi/content/full/3/6/e1603203/DC1

fig. S1. Anchoring monomer–mediated interfacial polymerization.
fig. S2. SEM image of topological particles and composite film.
fig. S3. Time-dependent morphology and size evolution of typical crescent moon–shaped PSDVB ⊃ PAA particles.
fig. S4. Schematic illustration of the initial configuration of the simulations.
fig. S5. Illustration of the reaction process controlled by the reaction probability and reaction radius in the copolymerization.
fig. S6. The influence of the concentration of AA on the morphology of Janus particle.
fig. S7. The influence of the number of hydrophobic monomer beads on the morphology of particle.
fig. S8. Characterization of crescent moon–shaped PSDVB ⊃ PHEA particles.
fig. S9. Characterization of crescent moon–shaped PSDVB ⊃ PMAH Janus particles.
fig. S10. Characterization of crescent moon–shaped PSDVB ⊃ PHEMA particles.
fig. S11. Characterization of crescent moon–shaped PSDVB ⊃ PMA Janus particles.
fig. S12. Characterization of crescent moon–shaped PSDVB ⊃ PIA particles.
fig. S13. Characterization of crescent moon–shaped PSDVB ⊃ PAM particles.
fig. S14. Characterization of crescent moon–shaped PSDVB ⊃ PNIPAM particles.
fig. S15. Characterization of crescent moon–shaped PSDVB ⊃ PMAM particles.
fig. S16. Ag nanoparticle characterization.

fig. S17. Fe_3O_4 nanoparticle characterization.
fig. S18. SEM images of the Janus particles capture and recognize spherical PS particles and live bacteria.
table S1. Dissipative particle dynamics simulation interaction parameters between different types of beads.
movie S1. Polymerization of 15 min.

REFERENCES AND NOTES

1. R. M. Pitman, C. D. Tweedle, M. J. Cohen, Branching of central neurons: Intracellular cobalt injection for light and electron microscopy. *Science* **176**, 412–414 (1972).
2. Y. J. Lee, H. Yi, W.-J. Kim, K. Kang, D. S. Yun, M. S. Strano, G. Ceder, A. M. Belcher, Fabricating genetically engineered high-power lithium-ion batteries using multiple virus genes. *Science* **324**, 1051–1055 (2009).
3. J. A. Lukin, G. Kontaxis, V. Simplaceanu, Y. Yuan, A. Bax, C. Ho, Quaternary structure of hemoglobin in solution. *Proc. Natl. Acad. Sci. U.S.A.* **100**, 517–520 (2003).
4. M. F. Perutz, M. G. Rossmann, A. F. Cullis, H. Muirhead, G. Will, A. C. T. North, Structure of haemoglobin: A three-dimensional Fourier synthesis at 5.5-Å. resolution, obtained by X-ray analysis. *Nature* **185**, 416–422 (1960).
5. A. Tromans, Cell biology: Asymmetry in action. *Nature* **411**, 33 (2001).
6. C. Huang, G. Yang, Q. Ha, J. Meng, S. Wang, Multifunctional "smart" particles engineered from live immunocytes: Toward capture and release of cancer cells. *Adv. Mater.* **27**, 310–313 (2015).
7. S. C. Glotzer, Some assembly required. *Science* **306**, 419–420 (2004).
8. S. Zhang, Fabrication of novel biomaterials through molecular self-assembly. *Nat. Biotechnol.* **21**, 1171–1178 (2003).
9. Y. Wang, D. R. Breed, V. N. Manoharan, L. Feng, A. D. Hollingsworth, M. Weck, D. J. Pine, Colloids with valence and specific directional bonding. *Nature* **491**, 51–55 (2012).
10. R. Dreyfus, J. Baudry, M. L. Roper, M. Fermigier, H. A. Stone, J. Bibette, Microscopic artificial swimmers. *Nature* **437**, 862–865 (2005).
11. D. A. Wilson, R. J. M. Nolte, J. C. M. van Hest, Autonomous movement of platinum-loaded stomatocytes. *Nat. Chem.* **4**, 268–274 (2012).
12. H. Park, N. Heldman, P. Rebentrost, L. Abbondanza, A. Iagatti, A. Alessi, B. Patrizi, M. Salvalaggio, L. Bussotti,M. Mohseni, F. Caruso, H. C. Johnsen, R. Fusco, P. Foggi, P. F. Scudo, S. Lloyd, A. M. Belcher, Enhanced energy transport in genetically engineered excitonic networks. *Nat. Mater.* **15**, 211–216 (2016).
13. J. Ugelstad, L. Söderberg, A. Berge, J. Bergström, Monodisperse polymer particles-a step forward for chromatography. *Nature* **303**, 95–96 (1983).
14. I. Piirma, *Emulsion Polymerization* (Academic Press, 1982).
15. C. S. Chern, *Principles and Applications of Emulsion Polymerization* (Wiley, 2008).
16. M. Okubo, T. Fujibayashi, M. Yamada, H. Minami, Micron-sized, monodisperse, snowman/confetti-shaped polymer particles by seeded dispersion polymerization. *Colloid Polym. Sci.* **283**, 1041–1045 (2005).
17. J.-W. Kim, R. J. Larsen, D. A Weitz, Uniform nonspherical colloidal particles with tunable shapes. *Adv. Mater.* **19**, 2005–2009 (2007).
18. W. D. Harkins, A general theory of the mechanism of emulsion polymerization. *J. Am. Chem. Soc.* **69**, 1428–1444 (1947).
19. W. V. Smith, R. H. Ewart, Kinetics of emulsion polymerization. *J. Chem. Phys.* **16**, 592–599 (1948).
20. J. Ugelstad, M. S. El-Aasser, J. W. Vanderhoff, Emulsion polymerization: Initiation of polymerization in monomer droplets. *J. Polym. Sci. Part C Polym. Lett.* **11**, 503–513 (1973).
21. W. V. Smith, The kinetics of styrene emulsion polymerization. *J. Am. Chem. Soc.* **70**, 3695–3702 (1948).
22. H. Ni, Y. Du, G. Ma, M. Nagai, S. Omi, Mechanism of soap-free emulsion polymerization of styrene and 4-vinylpyridine: Characteristics of reaction in the monomer phase, aqueous phase, and their interface. *Macromolecules* **34**, 6577–6585 (2001).
23. H. Sheu, M. El-Aasser, J. Vanderhoff, Phase separation in polystyrene latex interpenetrating polymer networks. *J. Polym. Sci. Part A Polym. Chem.* **28**, 629–651 (1990).
24. G. W. Poehlein, R. H. Ottewill, J. W. Goodwin, *Science and Technology of Polymer Colloids* (Springer, 1983), pp 51–59.
25. P. J. Flory, *Principles of Polymer Chemistry* (Cornell Univ. Press, 1953).
26. M. Morton, S. Kaizerman, M. W. Altier, Swelling of latex particles. *J. Colloid Sci.* **9**, 300–312 (1954).
27. H. Liu, H.-J. Qian, Y. Zhao, Z.-Y. Lu, Dissipative particle dynamics simulation study on the binary mixture phase separation coupled with polymerization. *J. Chem. Phys.* **127**, 144903 (2007).
28. H. Liu, M. Li, Z.-Y. Lu, Z. G. Zhang, C.-C. Sun, Influence of surface-initiated polymerization rate and initiator density on the properties of polymer brushes. *Macromolecules* **42**, 2863–2872 (2009).
29. R. D. Groot, P. B. Warren, Dissipative particle dynamics: Bridging the gap between atomistic and mesoscopic simulation. *J. Chem. Phys.* **107**, 4423–4435 (1997).
30. P. Español, P. Warren, Statistical mechanics of dissipative particle dynamics. *Europhys. Lett.* **30**, 191–196 (1995).
31. R. D. Groot, T. J. Madden, Dynamic simulation of diblock copolymer microphase separation. *J. Chem. Phys.* **108**, 8713–8724 (1998).
32. H. Liu, Y. L. Zhu, J. Zhang, Z. Y. Lu, Z. Y. Sun, Influence of grafting surface curvature on chain polydispersity and molecular weight in concave surface-initiated polymerization. *ACS Macro Lett.* **1**, 1249–1253 (2012).
33. Y. H. Xue, Y. L. Zhu, W. Quan, F. H. Qu, C. Han, J. T. Fan, H. Liu, Polymer-grafted nanoparticles prepared by surface-initiated polymerization: The characterization of polymer chain conformation, grafting density and polydispersity correlated to the grafting surface curvature. *Phys. Chem. Chem. Phys.* **15**, 15356–15364 (2013).
34. H. Liu, M. Li, Z. Y. Lu, Z. G. Zhang, C. C. Sun, T. Cu, Multiscale simulation study on the curing reaction and the network structure in a typical epoxy system. *Macromolecules* **44**, 8650–8660 (2011).
35. Y. L. Zhu, H. Liu, Z. W. Li, H. J. Qian, G. Milano, Z. Y. Lu, GALAMOST: GPU-accelerated large-scale molecular simulation toolkit. *J. Comput. Chem.* **34**, 2197–2211 (2013).
36. S. Sacanna, M. Korpics, K. Rodriguez, L. Colón-Meléndez, S. H. Kim, D. J. Pine, G. R. Yi, Shaping colloids for self-assembly. *Nat. Commun.* **4**, 1688 (2013).
37. S. H. Im, U. Jeong, Y. Xia, Polymer hollow particles with controllable holes in their surfaces, *Nat. Mater.* **4**, 671–675 (2005).
38. D. J. Kraft, J. Groenewold, W. K. Kegel, Colloidal molecules with well-controlled bond angles. *Soft Matter* **5**, 3823–3826 (2009).
39. C. H. J. Evers, J. A. Luiken, P. G. Bolhuis, W. K. Kegel, Self-assembly of microcapsules via colloidal bond hybridization and anisotropy. *Nature* **534**, 364–368 (2016).
40. S. H. Hu, X. Gao, Nanocomposites with spatially separated functionalities for combined imaging and magnetolytic therapy. *J. Am. Chem. Soc.* **132**, 7234–7237 (2010).
41. S. H. Kim, A. Abbaspourrad, D. A. Weitz, Amphiphilic crescent-moon-shaped microparticles formed by selective adsorption of colloids. *J. Am. Chem. Soc.* **133**, 5516–5524 (2011).
42. T. Nisisako, T. Torii, T. Takahashi, Y. Takizawa, Synthesis of monodisperse bicolored Janus particles with electrical anisotropy using a microfluidic co-flow system. *Adv. Mater.* **18**, 1152–1156 (2006).
43. J. R. Howse, R. A. L. Jones, A. J. Ryan, T. Gough, R. Vafabakhsh, R. Golestanian, Self-motile colloidal particles: From directed propulsion to random walk. *Phys. Rev. Lett.* **99**, 048102 (2007).
44. A. Brown, W. Poon, Ionic effects in self-propelled Pt-coated Janus swimmers. *Soft Matter* **10**, 4016–4027 (2014).
45. J. Choi, Y. Zhao, D. Zhang, S. Chien, Y. H. Lo, Patterned fluorescent particles as nanoprobes for the investigation of molecular interactions. *Nano Lett.* **3**, 995–1000 (2003).
46. L. Hong, S. Jiang, S. Granick, Simple method to produce Janus colloidal particles in large quantity. *Langmuir* **22**, 9495–9499 (2006).
47. K. H. Roh, D. C. Martin, J. Lahann, Biphasic Janus particles with nanoscale anisotropy. *Nat. Mater.* **4**, 759–763 (2005).
48. R. Erhardt, M. Zhang, A. Böker, H. Zettl, C. Abetz, P. Frederik, G. Krausch, V. Abetz, A. H. E. Müller, Amphiphilic Janus micelles with polystyrene and poly(methacrylic acid) hemispheres. *J. Am. Chem. Soc.* **125**, 3260–3267 (2003).
49. F. Liang, C. Zhang, Z. Yang, Rational design and synthesis of Janus composites. *Adv. Mater.* **26**, 6944–6949 (2014).
50. M. Chen, Y. G. Feng, X. Wang, T. C. Li, J. Y. Zhang, D. J. Qian, Silver nanoparticles capped by oleylamine: Formation, growth, and self-organization. *Langmuir* **23**, 5296–5304 (2007).
51. Z. Xu, C. Shen, Y. Hou, H. Gao, S. Sun, Oleylamine as both reducing agent and stabilizer in a facile synthesis of magnetite nanoparticles. *Chem. Mater.* **21**, 1778–1780 (2009).

Acknowledgments

Funding: This study was supported by the National Natural Science Foundation (21425314, 21504098, 21474042, 21534004, 21501184, 21434009, and 21421061), the Key Research Program of the Chinese Academy of Sciences (KJZD-EW-M01), the Ministry of Science and Technology of China (2013YQ190467), the Beijing Municipal Science and Technology Commission (Z161100000116037), and the Top-Notch Young Talents Program of China.
Author contributions: J.-B.F. and S.W. conceived and designed the study. J.-B.F. and Y.S. performed most of the experiments and characterization of Janus particles. Hong Liu and Z.L. performed the computer simulation. L.G. performed the STEM images. J.-B.F. and S.W. wrote the manuscript. L.J., Y.S., F.Z., Hongliang Liu, and J.M. revised the manuscript. All authors discussed the results and commented on the manuscript. **Competing interests:** The authors declare that they have no competing interests. **Data and materials availability:** All data needed to evaluate the conclusions in the paper are present in the paper and/or the Supplementary Materials. Additional data related to this paper may be requested from the authors.

Submitted 5 January 2017
Accepted 25 April 2017
Published 21 June 2017
10.1126/sciadv.1603203

Citation: J.-B. Fan, Y. Song, H. Liu, Z. Lu, F. Zhang, H. Liu, J. Meng, L. Gu, S. Wang, L. Jiang, A general strategy to synthesize chemically and topologically anisotropic Janus particles. *Sci. Adv.* **3**, e1603203 (2017).